ACS APPLIED ELECTRONIC MATERIALS

pubs.acs.org/acsaelm

Spotlight on Applications

Electrochemical Exfoliation and Laser Processing Bring Minerals to Advanced Electronic Applications

Elizaveta Dogadina, Raul D. Rodriguez,* and Evgeniya Sheremet

Cite This: https://doi.org/10.1021/acsaelm.5c02186

Read Online

ACCESS | Metrics & More | Article Recommendations

ABSTRACT: While 2D materials possess exceptional properties, their practical use remains limited by a critical gap: the lack of scalable manufacturing methods to bridge laboratory synthesis and industrial production. Here, we propose a "mineral-to-device" workflow that combines electrochemical exfoliation (ECE) and laser processing to create robust, flexible, and implantable electronics directly from natural minerals. We call this the "Ink and Pen" concept: it starts with a green, scalable ECE process to yield high-quality, diazonium-functionalized graphene inks ("The Ink") and uses laser processing ("The Pen") as a maskless tool to pattern and integrate these materials onto polymers and ceramic-coated titanium. To demonstrate the versatility of this approach, we fabricated mechanically robust circuits, multimodal sensors, and biocompatible electronics for medical implants that function reliably under physiological conditions. This technology offers a sustainable pathway for using diverse 2D minerals, paving the way for next-generation smart systems ranging from healthcare wearables to the Internet of Everything.

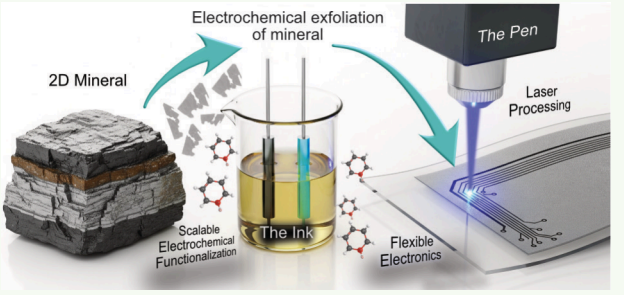

KEYWORDS: *laser processing, electrochemical exfoliation, 2D minerals, functionalized graphene, flexible electronics, wearable sensors, bioelectronics*

1. INTRODUCTION

The discovery of graphene through the mechanical exfoliation of the well-known 2D mineral graphite opened unprecedented opportunities in electronics, sensing, and energy applications.[1] In particular, 2D materials show unique advantages such as high charge carrier mobility, mechanical flexibility, and tunable electronic properties, which make them highly attractive for flexible and wearable devices.[2] However, the Nobel-prized "Scotch-tape method" remains fundamentally limited for practical applications.[3] To realize the transformative potential of 2D minerals in electronics, we need new manufacturing methods that are bridging the gap between laboratory-scale synthesis and industrial production.

Traditionally, mechanical exfoliation has remained the gold standard for isolating pristine, high-quality monolayers suitable for fundamental studies.[4] While our group has leveraged this technique to discover new phenomena in minerals, such as arsenic trisulfide (As_2S_3),[5] molybdenum disulfide (MoS_2),[6] and gallium selenide (GaSe),[7] mechanical exfoliation cannot support large-scale device manufacturing. To address this scalability challenge, electrochemical exfoliation (ECE) has emerged as one of the most promising approaches for creating a scalable 2D material "ink".[8] Works by Parvez[9] established the efficiency of ECE for producing high-quality graphene, while early studies by Hirsch demonstrated the power of diazonium chemistry for covalent functionalization.[10] Building on these fundamental synthesis methods, our group pioneered the specific strategy of integrating this diazonium-functionalized graphene (Mod-G) into electronic devices via laser processing.

Once the material is available as an ink, the next challenge is its integration into functional devices. Still, conventional lithographic and chemical patterning methods suffer from limitations, including complex processing, limited design flexibility, and high costs.[11,12] Laser processing, in contrast, provides a modern, maskless, and highly precise solution for writing, sintering,[13,14] and structuring[15] materials for fabricating flexible electronics on polymeric substrates on demand.[16] Seminal works have established two main paradigms: the laser-assisted reduction of graphene oxide (GO) films,[17] popularized by Kaner's group,[18] and the direct conversion of the polymer substrate itself into conductive laser-induced graphene (LIG), as demonstrated by Tour's group,[19] and further expanded for flexible sensors.[20,21] Beyond carbon, lasers are widely utilized

Received: October 15, 2025
Revised: February 5, 2026
Accepted: February 5, 2026

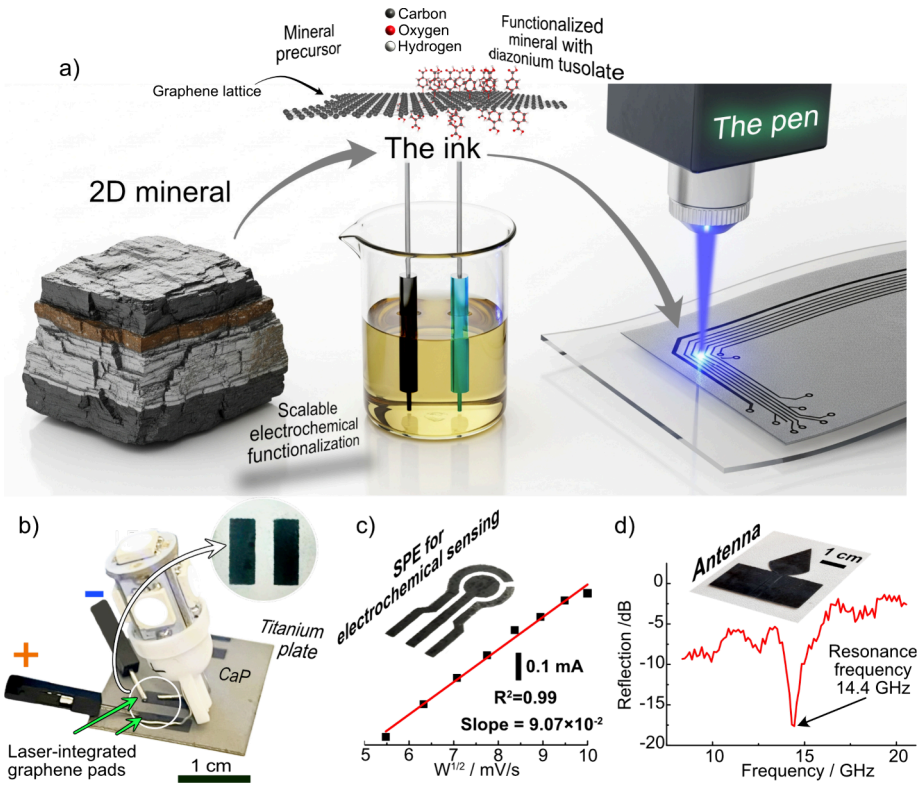

Figure 1. (a) Schematic illustration of the synergistic "Ink and Pen" workflow for fabricating advanced 2D material electronics. The process begins with a natural 2D mineral (e.g., graphite), which is converted into a high-quality, functionalized graphene "ink" via a scalable electrochemical process. A high-precision laser "pen" then directly writes and integrates this ink into a robust, conductive composite on a substrate to form a device. This versatile workflow enables a new generation of high-performance applications, including (b) biocompatible electronics on medical implant materials, (c) all-2D Ink screen-printed electrode (SPE) for electrochemical sensing, and (d) flexible high-frequency antennas for wireless communications. Panel b: Reproduced with permission from ref 27. Copyright 2025 American Chemical Society. Panels c and d: Reproduced with permission from ref 26. Copyright 2022 Elsevier.

to sinter and embed various nanomaterial inks, such as metal nanoparticles,[22] into thermoplastic matrices to create functional composites. Building on these advances, our group has demonstrated that lasers can process a wide spectrum of functional materials, ranging from GO on textiles,[23] to metal nanoparticles on polymers,[22] and even the upcycling of oil waste into conductive composites,[24] providing a fundamental understanding of the laser interaction mechanisms.[25]

In this Spotlight on Applications, we present a complete mineral-to-device workflow built on the unique synergy between the ECE process and high-precision laser processing. Unlike conventional methods, where synthesis and patterning are disconnected, our approach couples them: ECE provides an "ink", functionalized with diazonium salts, while the laser serves as a "digital pen" that simultaneously patterns, restores conductivity, and integrates this ink into the substrate. We demonstrate how this integrated approach enables a new generation of devices, from flexible multimodal sensors[26] to biocompatible implantable electronics that maintain functionality under physiological conditions.[27]

2. SYNERGISTIC WORKFLOW: A NEW PARADIGM FOR 2D MATERIAL FABRICATION

2.1. The "Ink": Scalable Production of Functionalized Graphene via Electrochemical Exfoliation

GO has long been valued for its combination of oxygen-containing functional groups, which transform graphene into a hydrophilic, easily dispersible material suitable for solution-based processing.[28] This functionalization allows GO to overcome many of the processing challenges associated with pristine graphene, enabling scalable, cost-effective production, which is crucial for industrial applications.[29] However, these advantages come at the cost of a hazardous chemical production process, typically requiring strong oxidants and generating significant chemical waste. To address these critical trade-offs, our approach introduces diazonium-functionalized graphene (Mod-G), an excellent alternative to GO.[30] We achieve this through a one-step ECE of graphite electrode in the presence of diazonium salts, which exfoliates graphite and functionalizes graphene sheets simultaneously, producing a stable, water-soluble "ink" enabling facile solution processing (Figure 1a). The one-step ECE mechanism involves the intercalation of sulfate anions into graphite layers, followed by gas-driven expansion from electrochemical decomposition of water and the release of nitrogen molecules from the diazonium species. Crucially, in situ-generated aryl radicals simultaneously functionalize the exfoliated sheets, stabilizing them against restacking and rendering them water-dispersible.[30] The remarkable stability of this dispersion arises from the formation of a robust solvation shell (hydration layer) around the hydrophilic functional groups grafted onto the graphene sheets. This solvent interface acts as a barrier that prevents the restacking of flakes due to the van der Waals attraction. Beyond graphite, the ECE approach can also be applied to other layered minerals (such as MoS_2[31,32] and stibnite[31,32]), enabling water-dispersible inks of diverse natural

https://doi.org/10.1021/acsaelm.5c02186
ACS Appl. Electron. Mater. XXXX, XXX, XXX−XXX

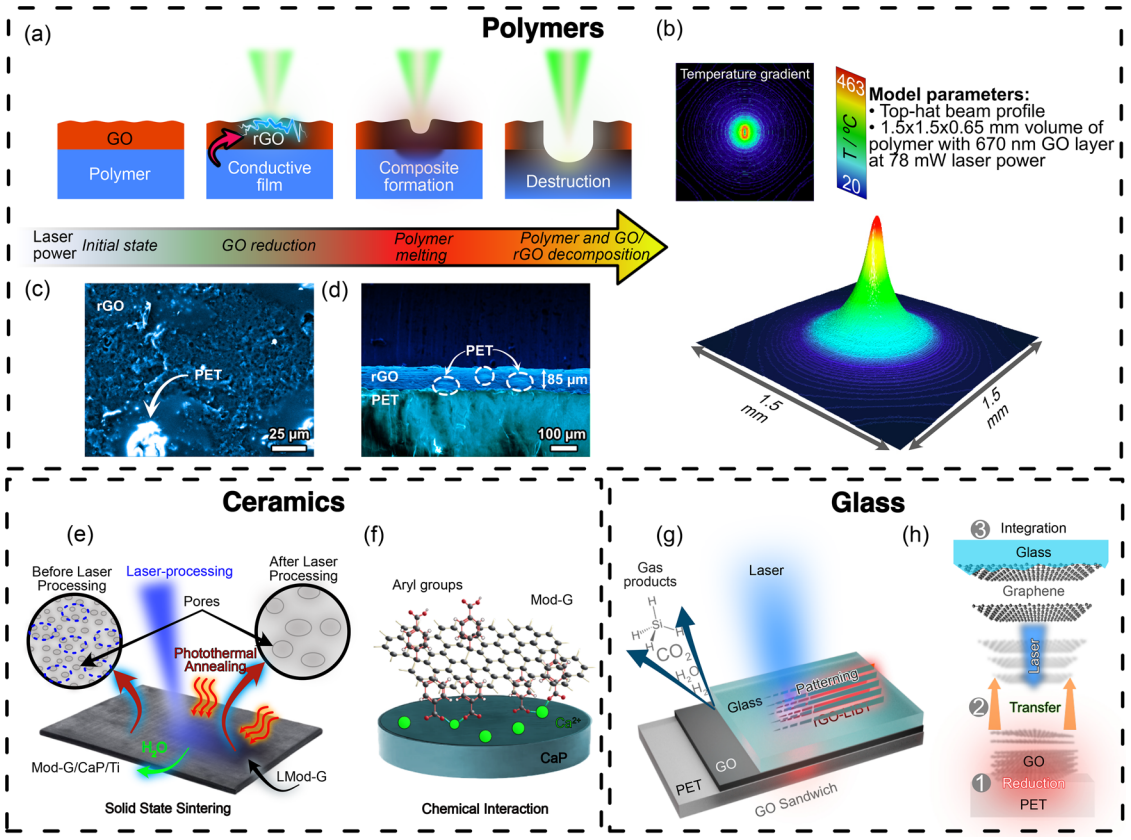

Figure 2. Laser processing applied to different substrates. (a) Evolution of thermal processing on GO/polymer interfaces depending on laser power. Reproduced with permission from ref 25. Copyright 2023 The Authors under Creative Commons CC-BY license, published by MDPI. (b) 3D temperature map obtained by computer modeling of polymer heating under the laser treatment. Reproduced with permission from ref 25. Copyright 2023 The Authors under the Creative Commons CC-BY license, published by MDPI. (c) SEM top-view image of rGO/polymer composite electrode. Reproduced with permission from ref 38. Copyright 2025 The Authors under the Creative Commons CC-BY license, published by MDPI. (d) Cross-sectional SEM image of rGO/polymer composite. Reproduced with permission from ref 38. Copyright 2025 The Authors under the Creative Commons CC-BY license, published by MDPI. (e) Composite formation mechanisms of Mod-G and CaP on Ti substrate via laser-induced photothermal annealing and sintering. Reproduced with permission from ref 27. Copyright 2025 American Chemical Society. (f) Composite formation mechanisms of Mod-G and CaP via chemical interaction between the functional carboxylic groups in Mod-G and Ca^{2+} ions in the CaP layer. Reproduced with permission from ref 27. Copyright 2025 American Chemical Society. (g) Illustration of the laser-induced graphene−glass composite by laser-induced backward transfer (LIBT). Reproduced with permission from ref 39. Copyright 2022 John Wiley and Sons. (h) During irradiation, the simultaneous GO reduction and H_2O and CO_2 gas release (1), graphene transfer (2), and its integration into the glass (3). Reproduced with permission from ref 39. Copyright 2022 John Wiley and Sons.

2D materials. Critical quality criteria for such inks include flake size, long-term aqueous stability (months) without surfactants, a monolayered structure, and high initial electrical resistance. The latter is crucial as it allows the laser to selectively restore conductivity, creating high-contrast patterns against the insulating background. Meeting these requirements makes ECE method superior to the liquid-phase exfoliation, since the harsh sonication typically results in a smaller and lower quality flake,[33] but the electrochemical driving force produces high-quality mineral sheets with larger lateral dimensions.[9]

Unlike traditional methods, such as the Hummers' method, this mild and greener electrochemical approach operates under ambient conditions and is readily scalable for large-volume production. Regarding safety management during scale-up, the specific arenediazonium tosylates used here are distinct from unstable diazo species; they are reported as safe, nonexplosive, and stable solids.[34] Compared to the explosion risks and toxic reagents (e.g., hydrazine) associated with conventional GO production and reduction,[35] this workflow offers a favorable safety outlook for industrial adoption, provided that their reactivity toward metals is properly managed.[36] Building on this safe and scalable foundation, our approach allows the fabrication of biocompatible implant electronics (Figure 1b) and flexible electronics (Figure 1c), including high-frequency antennas (Figure 1d).

2.2. The "Pen": Laser-Driven Composite Formation and Patterning

Building on the functionalized graphene ink, laser processing acts as an advanced materials integration technique, allowing the fabrication of novel composite materials. Laser processing achieves maskless, spatially selective patterning with tunable material properties through adjustable laser parameters. Typically, we operate with a laser spot size of ∼50 μm, allowing for the direct writing of intricate microcircuits. However, this resolution is defined by our optical setup and can be further improved. The laser power is adjusted between ∼10 mW (for partial reduction, favorable for sensing) and ∼500 mW (for maximal conductivity) on polymer substrates, and 1.6 W for conductive paths on ceramics, offering a wide processing window tailored to the specific application. Specifically, laser processing precisely removes the aryl groups

https://doi.org/10.1021/acsaelm.5c02186
ACS Appl. Electron. Mater. XXXX, XXX, XXX−XXX

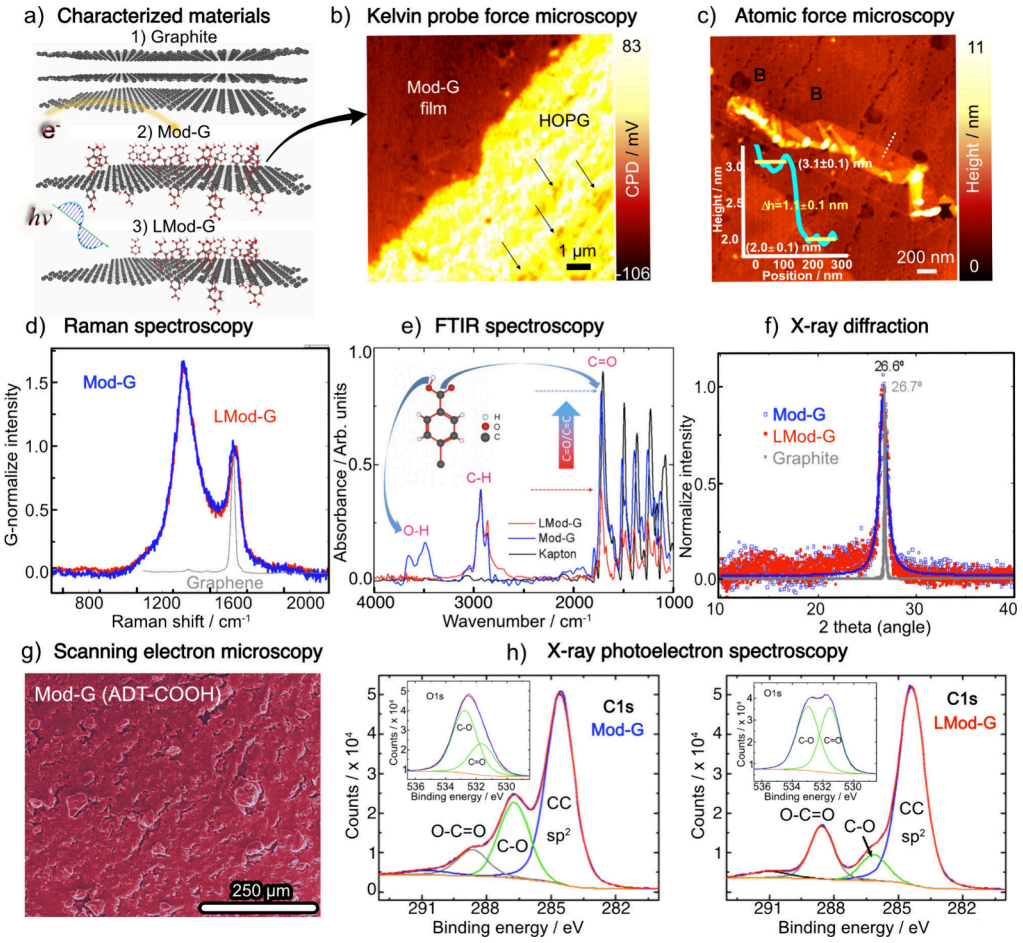

Figure 3. Material characterization techniques. (a) Schematics of the Mod-G generation from (i) a graphite precursor, (ii) aryl functionalization, and (iii) removal by laser irradiation. (b) KPFM image of the interface between a Mod-G film and HOPG obtained after drop-coating using a Mod-G dispersion obtained from ECE. (c) AFM zoom-in image on the lower-right side of panel b showing a monolayer graphene flake of about 1.1 nm thickness deduced from the cross-section in the inset. (d) Raman spectra of Mod-G and LMod-G. The Raman spectrum from single-layer graphene is included as a reference for purely sp^2 hybridized carbon. (e) FTIR spectra acquired from Mod-G on a Kapton substrate and an LMod-G. (f) X-ray diffractograms of Mod-G and LMod-G. The graphite result used as the reference for C═C sp^2 is taken from the RUFF Database, RRUFF ID: R050503.1. (g) SEM images of the Mod-G surface. (h) High-resolution spectra of C 1s regions before laser processing (Mod-G) and after (LMod-G), respectively. Reproduced with permission from ref 30. Copyright 2020 The Authors under a Creative Commons Attribution 3.0 Unported License, published by Royal Society of Chemistry.

covalently attached to the Mod-G, effectively restoring the conductive sp^2 carbon network, as demonstrated by Raman spectroscopy and X-ray photoelectron spectroscopy (XPS; see Section 2.3).

Acting as a light absorber similar to GO, Mod-G follows the same laser-induced thermal integration pathway. As illustrated in Figure 2a, applying laser energy to GO on polymer substrates such as polyethylene terephthalate (PET) induces a controllable evolution of thermal regimes. Initially, the graphene-based coating absorbs the optical energy, acting as a localized heater that triggers the removal of functional groups. With optimized power, heat transfer induces a shallow melt pool in the polymer substrate, where Benard-Marangoni convection drives the graphene flakes into the matrix. Crucially, this power must be balanced to avoid a 'destructive regime' in which excessive heat leads to polymer carbonization or ablation. Using a 438 nm diode laser in ambient air, we demonstrated that precise control of laser power enables fine-tuning of the melt depth, balancing polymer melting without inducing substrate ablation.[25,26] This process was confirmed by high-speed video imaging and supported by finite element method (FEM) simulations (Figure 2b).[25,26] Crucially, the laser parameters are optimized to operate within a specific thermal window. The local temperature is kept below the oxidative degradation threshold of Mod-G (<1000 °C),[26] which is significantly lower than the temperatures typically required to convert polymers into laser-induced graphene (>2000 °C).[37] This ensures that the polymer substrate is melted solely to facilitate embedding via Benard−Marangoni convection, without undergoing carbonization itself. While the polymer is in a molten state, the complex physical phenomena known as Benard−Marangoni convection occur and drive the dynamic mixing and integration between the molten polymer and graphene, enabling graphene to embed within the resolidified polymer.[38] This mechanism is expected to be similar to both forms of functionalized graphene - Mod-G and GO. For the case of GO, scanning electron microscopy (SEM) characterization reveal a smooth, homogeneous composite surface distinct from porous or carbonized features typical of laser-reduced GO alone, indicating effective polymer−graphene integration (Figure 1c,d). This integration significantly enhances the mechanical robustness and electrical

https://doi.org/10.1021/acsaelm.5c02186
ACS Appl. Electron. Mater. XXXX, XXX, XXX−XXX

conductivity of the composite, resulting in an ultrarobust, flexible material that can withstand bending, abrasion, and other mechanical stresses.

Extending this laser integration approach to biomedical implant materials such as calcium phosphate (CaP)-coated titanium, laser processing induces solid-state sintering of graphene with the CaP coating (Figure 2e).[27] Chemical interactions between graphene's functional groups (particularly carboxylic acid moieties) and Ca^{2+} ions in the CaP layer promote strong chemical bonding, contributing to mechanical durability and stable electrical pathways (Figure 2f).[27]

Similarly, the "pen" approach can be applied to glass substrates (Figure 2g), where a technique like laser-induced backward transfer (LIBT) has been successfully used to integrate GO, resulting in a robust composite (Figure 2h).[39]

This process is broadly applicable to various thermoplastic polymers, textiles, ceramic implant coatings, and glass. It facilitates the scalable, mask-free fabrication of graphene-based composites with tunable electrical and mechanical properties, making it well-suited for both flexible and rigid electronics and medical device fabrication. Practically, the ink is applied via drop-casting. A distinct advantage of this workflow is the "development" capability: the laser selectively integrates the graphene into the polymer/ceramic matrix, creating a robust pattern. Meanwhile, the nonirradiated material remains hydrophilic and water-soluble, allowing it to be simply washed away to reveal the predefined conductive circuit.

2.3. Advanced Characterization: Proving the Fundamentals

To ensure a deep understanding of the resulting graphene ink (Figure 3a) and laser-processed composites, a suite of advanced nanoscale characterization tools was employed. These techniques provide crucial insights into the fundamental physics and chemistry of the materials at the nanoscale.

Kelvin probe force microscopy (KPFM) (Figure 3b), for instance, offers direct evidence of graphene's functionalization with aryl groups (stage 1 → 2 in Figure 3a).[30] The shifts in surface potential detected between pristine graphite and Mod-G confirm a chemical functionalization that is both homogeneous and stable—a critical factor for achieving reproducible device fabrication. Aryl functionalization significantly improves the material's dispersibility and enables precise tuning of its electrical properties via controlled, laser-induced removal of functional groups. In addition, atomic force microscopy (AFM) images confirmed a monolayered nature of Mod-G (thickness of approximately 1.1 nm) (Figure 3c), which underlines the successful exfoliation and stability achieved by diazonium functionalization.

Raman spectroscopy (Figure 3d) allowed us to compare structural features of graphene, Mod-G, and its laser-treated counterpart, LMod-G. Both samples showed prominent D and G bands that closely resemble each other before and after laser processing. However, they differ significantly from the case of graphene, suggesting that laser processing likely introduces only chemical changes to the structure, resulting in a highly defective, conductive carbon network. We then tracked the chemical changes introduced during laser processing using Fourier transform infrared spectroscopy (FTIR) (Figure 3e). The disappearance of O−H and a significant decrease of C═O vibrational bands in LMod-G proved that the aryl groups had been effectively removed, implying a partial restoration of the graphene lattice.

In addition, we performed X-ray diffraction (XRD, Figure 3f) to compare Mod-G and LMod-G with pristine graphite. This analysis revealed that the material's graphitic structure was mostly preserved throughout both the chemical and laser processing stages. Specifically, the LMod-G material exhibited only a minor loss in crystallinity compared to the graphite standard. Further morphological and chemical characterization by SEM (Figure 3g) shows the surface uniformity of Mod-G, while high-resolution XPS (Figure 3h) quantitatively tracks the chemical evolution. The XPS spectra show a strong decrease in the C−O group after laser processing, with an increased fraction of sp^2 carbon, directly validating the conversion from functionalized to conductive graphene.

For composite materials, such as graphene integrated into CaP coatings on titanium implants, CSAFM combined with EDX confirms and explains the appearance of electrically conductive graphene networks. These techniques reveal a uniform distribution of electrical conductance across the surface covered by LMod-G, indicating uniform conductive pathways.[27] In addition, AFM and SEM imaging help to correlate morphological changes induced by laser processing, such as enlargement of pores and incorporation of graphene into the CaP matrices, thus confirming the robust nature of the composite interfaces.

While EDX provides elemental mapping, it does not provide information about chemical bonds and can not distinguish allotropes of the same element, for instance, graphene and amorphous carbon. Tip-enhanced Raman spectroscopy (TERS)[40] offers complementary advantages by combining chemical specificity with exceptional nanoscale spatial resolution (∼15−25 nm). Sheremet et al. demonstrated TERS' ability to differentiate GO, single-wall carbon nanotubes (CNTs), C_{60} fullerenes, and organic residues within a single sample with a ∼15 nm resolution. In other words, TERS overcomes the spatial resolution limitations of Raman spectroscopy, allowing for the resolution of closely intermixed components at the nanoscale.

In addition, TERS enables quantitative nanoscale strain mapping in two-dimensional materials, achieving high strain-sensitivity (∼1.4%). This enables the precise identification of strain localization at device-specific features such as wrinkles and edges during mechanical deformation. Thus, it provides a critical understanding of mechanical reliability and performance relevant for flexible electronics and wearable biomedical devices.

Finally, looking toward industrial quality control, the field is moving toward in situ and data-driven characterization. Dynamic light scattering (DLS) enables direct measurement of flake size distributions in the ink,[41] while electrochemical current monitoring (chronoamperometry) provides real-time feedback on the exfoliation rate.[42,43] Furthermore, machine learning (ML) strategies are emerging as powerful tools to automate the classification of flake thickness from simple optical images and to predict structure−property relationships from complex Raman data sets,[44] paving the way for systematic industrial standardization.

3. CASE STUDIES: FROM FLEXIBLE WEARABLES TO IMPLANTABLE BIOELECTRONICS

A material's technological importance is not just about its chemical and physical properties; it is about its practical impact. Our work has advanced laser-integrated graphene composites from a mere concept into a scalable platform for

https://doi.org/10.1021/acsaelm.5c02186
ACS Appl. Electron. Mater. XXXX, XXX, XXX−XXX

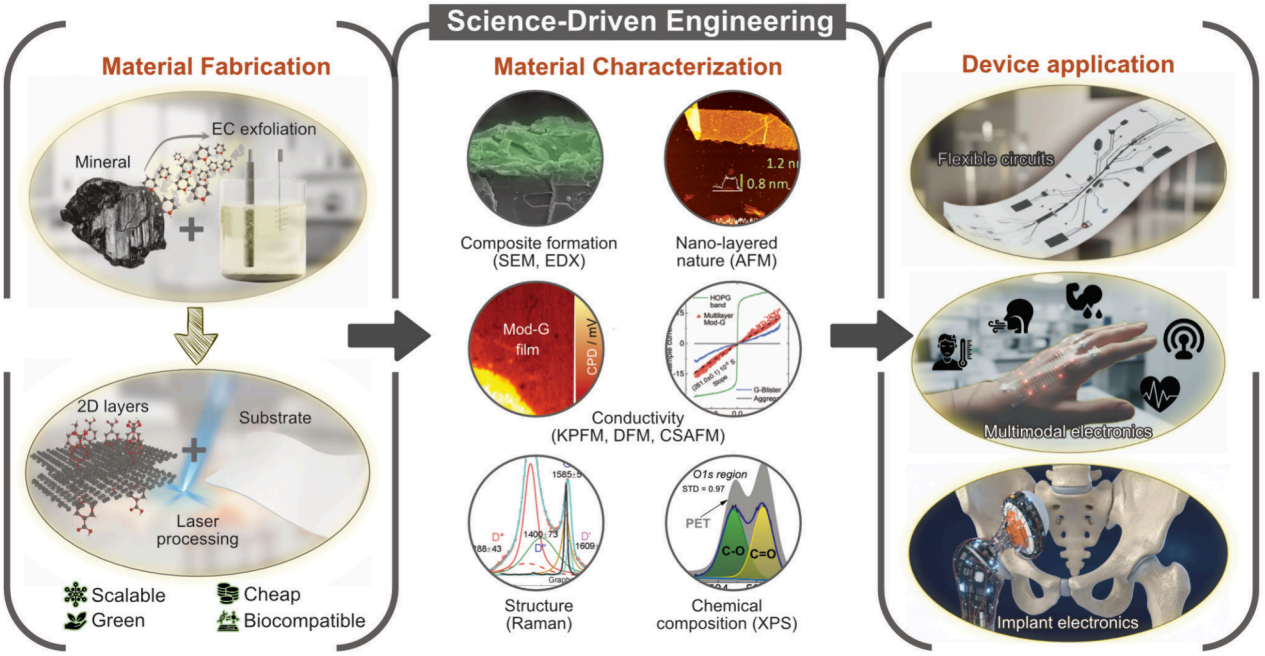

Figure 4. Science-driven engineering workflow that links material fabrication, material characterization, and device application for laser-integrated graphene composites from minerals.

new electronics. Characterization techniques provide the critical link between the engineered materials and their performance in flexible electronics (Figure 4). The material is so versatile that it is already being used in high-demand applications, including durable flexible circuits that outperform silver inks, and implantable electronics for the "Internet of the Body".

3.1. Flexible and Wearable Electronics

Flexible Electronic Circuits. The mechanical robustness of Mod-G laser-patterned circuits sets them apart from conventional conductive inks. On PET, 438 nm diode irradiation transforms insulating Mod-G coatings into 10−30 μm thick graphene/polymer composites with sheet resistance tuned from >MΩ/sq to tens/hundreds Ω/sq. Unlike ECE graphene without functionalization, which becomes porous under laser irradiation, LMod-G develops a smoother surface due to its polymer coating, indicating that melted PET serves as a matrix for graphene incorporation.[26] In this sense, laser processing is a universal approach, since it is capable of free-form patterning and compatible with different substrates. For example, LMod-G on Kapton circuits powered by solar cells (Figure 5a) operated continuously for weeks, maintaining over 98% of their initial current without failure after repeated 180° bending (Figure 5b,c). This reliability outperforms silver inks, which typically crack under similar conditions. PET circuits likewise exhibited minimal drift during extensive bending.[30] It demonstrates mechanical and electrical durability, which is due to the composite formation that suppresses crack initiation and delamination under strain. Cross-sectional SEM confirms the conductive layer is covered with PET, and high-speed imaging/thermal simulations show subsecond melting during the laser pass, explaining the fatigue resistance of the composite under cyclic loading.

Beyond simple circuits, these composites enable the direct fabrication of high-performance radio frequency (RF) components. To demonstrate the applicability of our material for high-frequency communications, we fabricated planar inverted cone antennas as a proof-of-concept. It is written directly on Mod-G/PET achieved performance with a −18 dB reflection coefficient at 14.4 GHz (full width at half-maximum ∼ 1 GHz), making them great for wearable and IoT applications.[26]

Multimodal Flexible Sensors. One of the most compelling advantages of our technology lies in its ability to create multifunctional sensor platforms from a single material. By precisely controlling laser processing parameters, we can tune local properties within the same composite to enable different sensing modalities on a single substrate.

Laser-written stripes on PET can act as *piezoresistive gauges*.[26] In three-point flexure tests, the relative resistance change ($\Delta R/R_0$) stabilized at 13−14% under bending radii from 15 to 50 mm and remained consistent over 10000 cycles. Calculated from the resistance response to applied strain, the gauge factor (GF) of these sensors is approximately 8.3, which surpasses conventional metallic strain gauges.[26] Such impressive stability and consistent response to deformation highlight the potential of laser-induced composite materials in mechanical sensing applications. One more demonstration is an *electrochemical sensor*, which could be engraved following screen-printed electrodes (SPE) geometry, where LMod-G acts as working, counter, and reference electrodes (Figure 5d), capable of detecting 0.1 M potassium ferro/ferricyanide.[26] It exhibits well-defined anodic and cathodic peaks exceeding 1 mA at 100 mV/s. After measurements, electrodes could be simply rinsed or briefly electrochemically cleaned and reused with reproducible performance, reflecting the chemically stable surface.

The composite material could also be used as a *temperature sensor* (Figure 5e). LMod-G/PET exhibits a monotonic decrease in resistance during cooling from 80 to 40 °C, with repeatable R-T sweeps. The response arises from thermal expansion of the composite, which increases separation

https://doi.org/10.1021/acsaelm.5c02186
ACS Appl. Electron. Mater. XXXX, XXX, XXX−XXX

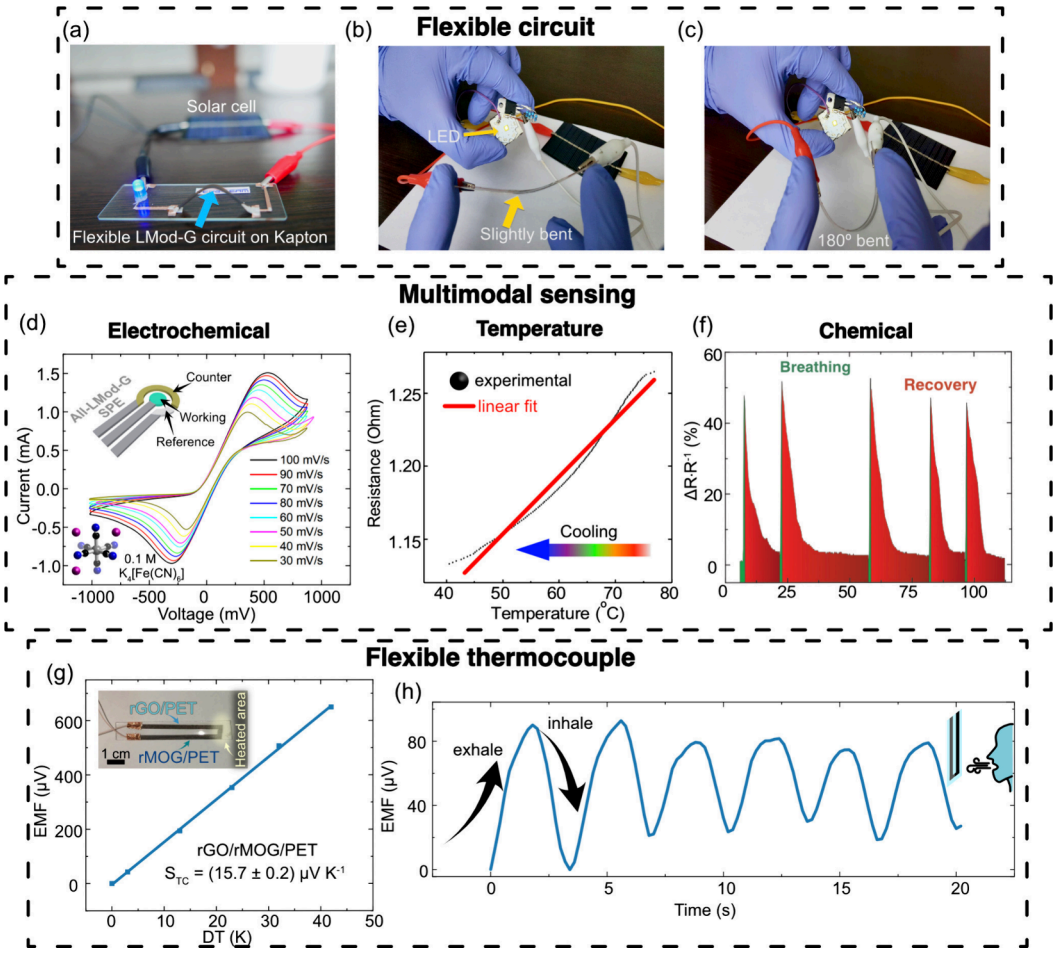

Figure 5. Flexible and wearable electronics. (a) Photograph of LMod-G on Kapton in a solar cell-powered circuit that operated 24/7 for several weeks with high current stability of over 98%. Pictures of an LMod-G flexible device on PET for (b) slightly bent and (c) 180° bent, while lighting another LED without drastic changes in conductance. Reproduced with permission from ref 30. Copyright 2020 The Authors under a Creative Commons Attribution 3.0 Unported License, published by Royal Society of Chemistry. (d) Demonstration of electrochemical sensor behavior by CV curves with the detection of 0.1 M $K_4[Fe(CN)_6]$ at different scan rates. Reproduced with permission from ref 26. Copyright 2022 Elsevier. (e) Temperature-resistance LMod-G sensor (cooling down). Reproduced with permission from ref 26. Copyright 2022 Elsevier. (f) Chemical sensor response to breathing. Reproduced with permission from ref 26. Copyright 2022 Elsevier. (g) Performance of the rGO-rMOG/PET thermocouple. Reproduced with permission from ref 45. Copyright 2025 Elsevier. (h) Response of the thermocouple to breathing under room conditions. Reproduced with permission from ref 45. Copyright 2025 Elsevier.

between conductive graphene layers inside the polymer matrix, which modulates conductivity.[26]

Low-power laser processing (~17 mW) yields partially integrated LMod-G films with sufficient defects and surface accessibility for *gas sensing*, enabling high chemiresistive responses (Figure 5f). LMod-G/PET responds within seconds to human breath and water vapor, with resistance increases driven by H_2O adsorption and swelling of the graphene layers, which expands interlayer spacing and results in increased resistance. Ethanol vapor likewise produces fast, reversible signals following the same mechanism. In contrast, the same devices show rapid resistance decreases upon exposure to dry gases such as CO_2 and Ar, as these gases displace adsorbed water molecules, drive moisture out of the film, and shrink the interlayer spacing. Sensors fabricated with higher laser power (more conductive, deeper composite) are markedly less responsive due to reduced accessible surface. Devices retain functionality over long intervals; the response to dry argon flow remained stable 12 months after initial use, underscoring durability and reusability.[26]

Paired LMod-G pads on PET function as *sweat/hydration sensors* by transducing ionic conductivity changes across the skin/electrode interface. In tests with NaCl solutions, the measured resistance decreased exponentially as NaCl concentration rose from 1 to 10%, reflecting the increase in electrolyte conductivity. The electrodes deliver rapid, repeatable signals without degradation under liquid exposure or finger pressure, owing to the embedded conductive network and stable surface after laser processing. The material's bacteriostatic nature further supports prolonged on-skin use.[26]

A single-step ECE Mod-G coating supports different implementations. The laser "sets" local properties for each function: low-power processing partially preserves surface functionality/porosity for chemical interaction, while higher-power densifies and maximizes conductivity for contact pads adjacent to sensing regions. Devices retain performance after extensive bending (including 180°), with gas sensors remaining stable even 1 year postfabrication, underscoring their suitability for wearables and health-monitoring systems built from a minerals-to-devices workflow that uses water-based dispersions and mask-free laser processing.[26]

https://doi.org/10.1021/acsaelm.5c02186
ACS Appl. Electron. Mater. XXXX, XXX, XXX−XXX

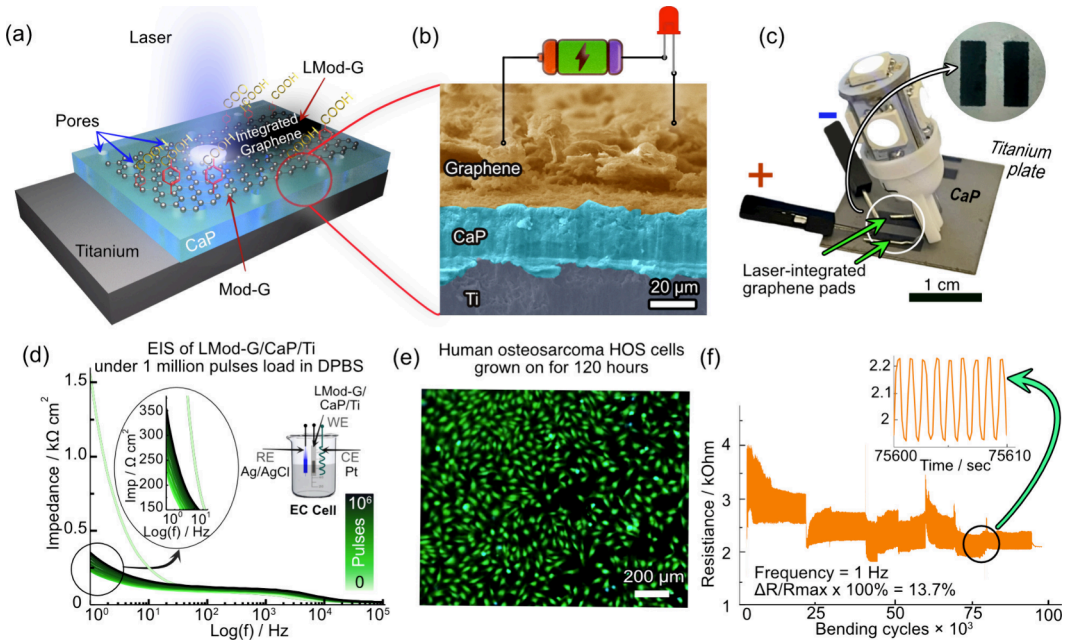

Figure 6. Implantable bioelectronics. (a) Schematic illustration of laser-induced graphene integration in CaP coating on titanium alloy. (b) Cross-sectional SEM image of the interface between graphene layers and CaP, color-coded red and blue, respectively. (c) Picture of a superbright LED being powered through the graphene composite conductors made on the CaP/Ti surface. (d) EIS of LMod-G/CaP/Ti under multipulse load. (e) Optical images of human osteosarcoma HOS cells grown on an LMod-G/CaP composite for 120 h. (f) Electrical resistance of an LMod-G/CaP/Ti sample as a function of bending cycles. The inset shows periodic changes in resistance over some cycles, with a variation of 13.7%. Reproduced with permission from ref 27. Copyright 2025 American Chemical Society.

Thermoelectric and Transistor Devices. Laser-based approach provides unprecedented control over the electronic properties of carbon-based composites. By selecting different starting materials, GO versus mildly oxidized graphene (MOG) laser processing can predictably create either p-type or n-type conductive composites.[45] This control stems from the different oxygen functional group concentrations in the precursors, which influence charge carrier type after laser-induced reduction.

This capability enables the fabrication of p−n junctions and complementary device architectures directly on flexible substrates. Laser-processed p- and n-type graphene composites on PET form *flexible thermocouples* (Figure 5g) by pairing rGO/PET (p-type) with rMOG/PET (n-type). The opposite signs of their Seebeck coefficients add constructively across the p−n junction, yielding a clear thermal dependence of the electromotive force (EMF) on temperature. Individually, rGO/PET and rMOG/PET exhibit Seebeck coefficients of approximately +6.6 and −3.9 μV/K, respectively. The combined rGO-rMOG device achieves a sensitivity of approximately 15−19 μV/K within the PET stability temperature range (up to ∼70 °C), with stable resistance confirming thermal robustness. Increasing conductivity can further raise output, demonstrated by resolving ∼50 μV oscillations during human breathing (Figure 5h).[45]

Furthermore, we fabricated *electrolyte-gated transistors (EGTs)* using electrochemically surface-activated composites. Those transistors exhibit ambipolar transfer curves with gate-tunable hole and electron conduction, achieving transconductances of up to ∼150 μS, depending on the carrier branch. Remarkably, these devices exhibit reversible p- to n-type transitions during operation due to ion-doping mechanisms, where K^+ penetration screens oxygen-containing groups and modifies their electron-acceptor character. This yields liquid-gated, n-type graphene/polymer channels with stable operation, expanding the composite's role from passive conductors to actively doped transistor channels suitable for low-voltage (bio)sensing.[45]

3.2. Implantable Bioelectronics

One more application is biocompatible electronics and sensors.[27] Direct laser integration of ECE Mod-G into CaP coatings on Ti-6Al-4 V alloy implant allows for a mineral-to-device workflow for implantable electronics that is biocompatible, mechanically robust, and long-term electrochemically stable in physiological media. Mod-G can be drop-casted onto microarc oxidized (MAO) CaP/Ti and laser processed to restore sp^2 conduction, sinter to porous CaP, and form bonded, low-impedance pathways (Figure 6a).

The laser-induced LMod-G/CaP composite forms via solid-state mechanisms that are fundamentally different from those of graphene/polymer integration. On the porous CaP, laser photothermally removes aryl groups ($sp^3 \rightarrow sp^2$ restoration) while inducing pore enlargement, water release, and partial recrystallization of amorphous CaP, which together drive graphene accumulation, sintering, and chemical coupling at the interface via carboxylate-Ca^{2+} interactions (Figure 2c,d).

Building on this mechanism, laser processing enables several smart implant-focused functions directly on CaP/Ti. Typical sheet resistance of layer-structured (Figure 6b) LMod-G/CaP/Ti is ∼1.3 kΩ/sq, remaining within the same order after cell culture, indicating stable performance under physiological conditions. This composite structure could act as an *electronic circuit*, which was confirmed by powering LEDs through it (Figure 6c).

Additionally, functionalization of the CaP coating with conductive LMod-G opens the possibility of applications as *stimulation electrodes* for bone tissue regeneration (Figure 6d).

https://doi.org/10.1021/acsaelm.5c02186
ACS Appl. Electron. Mater. XXXX, XXX, XXX−XXX

Under 1000000 bipolar pulses in phosphate-buffered saline (PBS), cyclic voltammetry and electrochemical impedance spectroscopy show initial changes that stabilize after ~200000 pulses, with low-frequency impedance deviations up to ~20%, supporting durable use for osteogenic electrical stimulation. The electrodes have excellent biocompatibility (Figure 6e). Generally, the cytotoxicity of graphene is a subject of debate, often linked to free-floating flakes that can physically pierce cell membranes with sharp edges or generate reactive oxygen species (ROS).[46] We previously demonstrated excellent biocompatibility for LrGO on PET,[47] given the identical laser-driven embedding mechanism, we expect the same for Mod-G composites. However, in our design, the graphene is integrated within the bioactive CaP matrix, which also minimizes the release of free particles and likely mitigates these toxicity mechanisms. While our in vitro results show excellent cell adhesion and proliferation for several cell lines, future clinical adoption will naturally require rigorous assessment of long-term in vivo responses. The LMod-G/CaP composite maintains conductivity for at least 12 weeks in PBS at 37 °C across pH 4.0−9.2, matching the typical bone healing timelines.

Also, LMod-G/CaP composites can act as a *bending sensor* to detect implant micromotion (Figure 6f). Under 100000 three-point bending cycles at 1 Hz with 2 mm deflection, the electrical response remains stable, showing periodic resistance modulation with a representative peak-to-peak variation of ~13−14% over individual cycles while avoiding failure. It thus supports continuous in situ readout of load transfer and healing progression.

The combination of biocompatibility, electrical functionality, and mechanical robustness positions laser-processed graphene-CaP composites as a transformative technology for implantable bioelectronics capable of real-time monitoring and therapeutic intervention. Furthermore, these implants could enable wireless communication with external medical systems, expanding their clinical potential.

4. CONCLUSIONS AND OUTLOOK

4.1. Conclusion

This work demonstrates a complete mineral-to-device workflow built on the powerful synergy between ECE and laser-processing technology. Our ECE method produces a high-quality, diazonium-functionalized graphene "ink" that serves as a greener and safer alternative to conventional GO. Using an advanced laser "pen", we transform this ink into ultrarobust, conductive composites by integration with polymer and ceramic substrates, such as PET, Kapton, and CaP-coated titanium.[48]

This integrated approach opened key breakthroughs in device applications, including the fabrication of robust flexible circuits and multimodal wearable sensors with bending, thermal, chemical, and electrochemical sensing. We have demonstrated tunable p- and n-type carbon/polymer composites that serve as the basis for advanced electronics such as highly sensitive thermocouples and electrolyte-gated transistors with reversible ambipolar switching. Furthermore, our technology creates biocompatible and highly stable electronic materials directly on medical implant surfaces, enabling real-time functionality under physiological conditions for extended durations.

Our applied advancements are underpinned by a deep fundamental understanding of the materials' nanoscale physics. Through various characterization techniques such as Raman spectroscopy, KPFM, CSAFM, XPS, and computer modeling, we achieve a comprehensive understanding of material properties, guiding rational design and optimization. This foundation of nanoscale insights ensures the reproducibility and high performance of our devices from ink production to final device fabrication.

4.2. Visionary Outlook

The synergistic workflow presented here is not an end point but a versatile platform for future innovations in materials science. The presented approach has the potential to be extended beyond graphite to a broad library of natural 2D minerals such as MoS_2 and others, promoting the fabrication of new composites with tunable electronic, optical, and catalytic properties. This expansion will open opportunities for customized materials with specific application functions.[48] Furthermore, drawing parallels with established techniques that convert biomass (e.g., lignin, cellulose) into graphitic structures via laser processing,[49,50] our method offers a complementary route. While biomass conversion relies on substrate precursors, our ink approach permits noncarbon circuit formation and integration onto noncarbonizable substrates (ceramics, glass). A promising future direction may be the convergence of these fields: creating fully sustainable electronics by printing mineral-derived inks onto biodegradable, laser-processed biomass substrates.

Looking forward, this approach paves the way for the development of fully integrated smart systems. These include the Internet of Bodies, where wearable and biocompatible implantable electronics continuously monitor and therapeutically interact with the human body.[51,52] Our workflow also lays the groundwork for next-generation, based on 2D minerals and textiles, which are capable of continuous health monitoring via embedded multimodal sensors designed to detect gestures, voice, pulse, or chemical biomarkers.[53]

Moreover, integrating this manufacturing process with Artificial Intelligence (AI) will enable autonomous optimization of both ECE and laser processing parameters. Such AI-based fabrication would offer on-demand production of devices with high precision and efficiency. Laser processing can turn other precursor materials, such as metal−organic frameworks, into novel functional composites for catalysis, sensing, and electronics.[54]

In summary, our work lights the way for the combination of green chemistry, advanced materials processing, and device engineering. We hope this work will help fuel future developments where scalable, customizable, and multifunctional 2D material-based electronics become widespread across healthcare, wearable technology, and beyond.

AUTHOR INFORMATION

Corresponding Author

Raul D. Rodriguez − *Tomsk Polytechnic University, Tomsk 634050, Russia; Shihezi University, Shihezi 832003 Xinjiang, China;* orcid.org/0000-0003-4016-1469; Email: rodriguez@tpu.ru

Authors

Elizaveta Dogadina − *Tomsk Polytechnic University, Tomsk 634050, Russia*

https://doi.org/10.1021/acsaelm.5c02186
ACS Appl. Electron. Mater. XXXX, XXX, XXX−XXX

Evgeniya Sheremet − *Tomsk Polytechnic University, Tomsk 634050, Russia;* orcid.org/0000-0003-3937-8628

Complete contact information is available at: https://pubs.acs.org/10.1021/acsaelm.5c02186

Notes

The authors declare no competing financial interest.

■ ACKNOWLEDGMENTS

The work was supported by the TPU development program Priority 2030. We thank Maxim Fatkullin and Pavel Postnikov for proofreading the manuscript.

■ REFERENCES

(1) Geim, A. K.; Novoselov, K. S. The rise of graphene. *Nat. Mater.* **2007**, *6*, 183−191.
(2) Hou, C. Boosting flexible electronics with integration of two-dimensional materials. *InfoMat* **2024**, *6*, e12555.
(3) Huang, Y.; et al. Universal mechanical exfoliation of large-area 2D crystals. *Nat. Commun.* **2020**, *11*, 2453.
(4) Yi, M.; Shen, Z. A review on mechanical exfoliation for the scalable production of graphene. *J. Mater. Chem. A Mater. Energy Sustain.* **2015**, *3*, 11700−11715.
(5) Garcia, A.; et al. Modulated photoresponse in a naturally-occurring two-dimensional material. *Appl. Mater. Today* **2025**, *42*, 102592.
(6) Rahaman, M.; et al. Highly Localized Strain in a MoS/Au Heterostructure Revealed by Tip-Enhanced Raman Spectroscopy. *Nano Lett.* **2017**, *17*, 6027−6033.
(7) Rodriguez, R. D.; et al. Selective Raman modes and strong photoluminescence of gallium selenide flakes on sp2 carbon. *J. Vac. Sci. Technol. B* **2014**, *32*, 04E106.
(8) Song, O.; Kang, J. Solution-processed 2D materials for electronic applications. *ACS Appl. Electron. Mater.* **2023**, *5*, 1335.
(9) Parvez, K.; et al. Exfoliation of graphite into graphene in aqueous solutions of inorganic salts. *J. Am. Chem. Soc.* **2014**, *136*, 6083−6091.
(10) Englert, J. M.; et al. Covalent bulk functionalization of graphene. *Nat. Chem.* **2011**, *3*, 279−286.
(11) Shi, Y.; et al. Damage-free LED lithography for atomically thin 2D material devices. *Sci. Rep* **2023**, *13*, 2583.
(12) Zhang, Y. 2D material integrated photonics: Toward industrial manufacturing and commercialization. *APL Photonics* **2025**, *10*, 040903.
(13) Xu, K.; et al. An in-situ hybrid laser-induced integrated sensor system with antioxidative copper. *Int. J. Extrem. Manuf.* **2024**, *6*, 065501.
(14) Hou, Y.; et al. A laser-induced wide-range thin-film temperature sensor without additional anti-oxidative encapsulations. *Int. J. Extrem. Manuf.* **2025**, *7*, 065508.
(15) Cai, Z.; et al. Bio-inspired hybrid laser direct writing of interfacial adhesion for universal functional coatings. *Adv. Funct. Mater.* **2024**, *34*, 2408354.
(16) Pinheiro, T.; et al. Direct Laser Writing: From Materials Synthesis and Conversion to Electronic Device Processing. *Adv. Mater.* **2024**, *36*, No. 2402014.
(17) Zhang, Y.; et al. Direct imprinting of microcircuits on graphene oxides film by femtosecond laser reduction. *Nano Today* **2010**, *5*, 15−20.
(18) El-Kady, M. F.; Strong, V.; Dubin, S.; Kaner, R. B. Laser scribing of high-performance and flexible graphene-based electrochemical capacitors. *Science* **2012**, *335*, 1326−1330.
(19) Lin, J.; et al. Laser-induced porous graphene films from commercial polymers. *Nat. Commun.* **2014**, *5*, 5714.
(20) Yu, H. Laser-induced direct graphene patterning: from formation mechanism to flexible applications. *Soft Sci.* **2023**, *3*, 4.
(21) Yue, Y.; Li, X.; Zhao, Z.; Wang, H.; Guo, X. Stretchable flexible sensors for smart tires based on laser-induced graphene technology. *Soft Sci.* **2023**, *3*, 13.
(22) Rodriguez, R. D.; et al. Ultra-robust flexible electronics by laser-driven polymer-nanomaterials integration. *Adv. Funct. Mater.* **2021**, *31*, 2008818.
(23) Fatkullin, M.; et al. Smart Graphene Textiles for Biopotential Monitoring: Laser-Tailored Electrochemical Property Enhancement. *ACS Sens* **2024**, *9*, 1809−1819.
(24) Petrov, I.; Rodriguez, R. D.; Frantsina, E.; Grinko, A.; Sheremet, E. Transforming oil waste into highly conductive composites: Enabling flexible electronics through laser processing of asphaltenes. *Adv. Compos. Hybrid Mater.* **2024**, *7*, 41.
(25) Abyzova, E. Universal Approach to Integrating Reduced Graphene Oxide into Polymer Electronics. *Polymers (Basel)* **2023**, *15*, 4622.
(26) Lipovka, A.; et al. Photoinduced flexible graphene/polymer nanocomposites: Design, formation mechanism, and properties engineering. *Carbon* **2022**, *194*, 154−161.
(27) Dogadina, E.; et al. Integration of Graphene into Calcium Phosphate Coating for Implant Electronics. *ACS Appl. Mater. Interfaces* **2025**, *17*, 13527−13537.
(28) Ikram, R.; Jan, B. M.; Ahmad, W. An overview of industrial scalable production of graphene oxide and analytical approaches for synthesis and characterization. *J. Mater. Res. Technol.* **2020**, *9*, 11587−11610.
(29) Nishina, Y. Mass Production of Graphene Oxide Beyond the Laboratory: Bridging the Gap Between Academic Research and Industry. *ACS Nano* **2024**, *18*, 33264−33275.
(30) Rodriguez, R. D.; et al. Beyond graphene oxide: laser engineering functionalized graphene for flexible electronics. *Mater. Horiz.* **2020**, *7*, 1030−1041.
(31) Zhang, P.; et al. Electrochemically Exfoliated High-Quality 2H-MoS for Multiflake Thin Film Flexible Biosensors. *Small* **2019**, *15*, No. 1901265.
(32) Li, J.; et al. Electrochemical exfoliation of naturally occurring layered mineral Stibnite (Sb_2S_3) for highly sensitive and fast room-temperature acetone sensing. *Adv. Mater. Interfaces* **2022**, *9*, 2200605.
(33) Narayan, R.; Kim, S. O. Surfactant mediated liquid phase exfoliation of graphene. *Nano Converg* **2015**, *2*, 20.
(34) Filimonov, V. D.; et al. Unusually stable, versatile, and pure arenediazonium tosylates: their preparation, structures, and synthetic applicability. *Org. Lett.* **2008**, *10*, 3961−3964.
(35) Losic, D.; Farivar, F.; Yap, P. L.; Tung, T. T.; Nine, M. J. New insights on energetic properties of graphene oxide (GO) materials and their safety and environmental risks. *Sci. Total Environ.* **2022**, *848*, 157743.
(36) Sheng, M.; Frurip, D.; Gorman, D. Reactive chemical hazards of diazonium salts. *J. Loss Prev. Process Ind.* **2015**, *38*, 114−118.
(37) Vashisth, A.; et al. ReaxFF simulations of laser-induced graphene (LIG) formation for multifunctional polymer nanocomposites. *ACS Appl. Nano Mater.* **2020**, *3*, 1881−1890.
(38) Fatkullin, M. Electrochemical Switching of Laser-Induced Graphene/Polymer Composites for Tunable Electronics. *Polymers (Basel)* **2025**, *17*, 192.
(39) Rodriguez, R. D.; et al. Laser-Engineered Multifunctional Graphene-Glass Electronics. *Adv. Mater.* **2022**, *34*, No. 2206877.
(40) Sheremet, E.; et al. Nanoscale imaging and identification of a four-component carbon sample. *Carbon N. Y.* **2016**, *96*, 588−593.
(41) Lotya, M.; Rakovich, A.; Donegan, J. F.; Coleman, J. N. Measuring the lateral size of liquid-exfoliated nanosheets with dynamic light scattering. *Nanotechnology* **2013**, *24*, 265703.
(42) Liu, F.; et al. Synthesis of graphene materials by electrochemical exfoliation: Recent progress and future potential. *Carbon Energy* **2019**, *1*, 173−199.
(43) Ljubek, G.; Čapeta, D.; Šrut Rakić, I.; Kraljić Roković, M. Energetically efficient and electrochemically tuneable exfoliation of graphite: process monitoring and product characterization. *J. Mater. Sci.* **2021**, *56*, 10859−10875.

(44) Yang, E. Machine Learning-Assisted Identification of Single-Layer Graphene via Color Variation Analysis. *Nanomaterials (Basel)* **2024**, *14*, 183.
(45) Petrov, I.; et al. Laser-induced p- and n-type graphene composites for flexible electronics. *Surf. Interfaces* **2025**, *68*, 106666.
(46) Liao, C.; Li, Y.; Tjong, S. C. Graphene Nanomaterials: Synthesis, Biocompatibility, and Cytotoxicity. *Int. J. Mol. Sci.* **2018**, *19*, 3564.
(47) Murastov, G.; et al. Flexible and water-stable graphene-based electrodes for long-term use in bioelectronics. *Biosens Bioelectron* **2020**, *166*, 112426.
(48) Zhao, M.; Casiraghi, C.; Parvez, K. Electrochemical exfoliation of 2D materials beyond graphene. *Chem. Soc. Rev.* **2024**, *53*, 3036−3064.
(49) Ye, R. Laser-Induced Graphene Formation on Wood. *Adv. Mater.* **2017**, *29*, 1702211.
(50) Chyan, Y.; et al. Laser-Induced Graphene by Multiple Lasing: Toward Electronics on Cloth, Paper, and Food. *ACS Nano* **2018**, *12*, 2176−2183.
(51) Kim, H.; Seong, S.; Gong, X. Heterostructure engineering of solution-processable semiconductors for wearable optoelectronics. *ACS Appl. Electron. Mater.* **2023**, *5*, 5278−5290.
(52) Baek, S.; Jo, Y.; Lee, Y.; Kwon, J.; Jung, S. Design and integration of organic printed thin-film transistor-based soft biosensors for wearable applications. *ACS Appl. Electron. Mater.* **2024**, *6*, 7657.
(53) Lipovka, A.; et al. Textile Electronics with Laser-Induced Graphene/Polymer Hybrid Fibers. *ACS Appl. Mater. Interfaces* **2023**, *15*, 38946−38955.
(54) Tran, T.-H.; et al. Laser-induced transformation of ZIF-8 into highly luminescent N-doped nanocarbons for flexible sensors. *Adv. Opt. Mater.* **2024**, DOI: 10.1002/adom.202401758.

https://doi.org/10.1021/acsaelm.5c02186
ACS Appl. Electron. Mater. XXXX, XXX, XXX−XXX